Intrinsic Electric Oscillations of Ovonic Devices towards the TeraHertz Limit

2015 J. Phys.: Conf. Ser. 647 012021

(http://iopscience.iop.org/1742-6596/647/1/012021)

Intrinsic Electric Oscillations of Ovonic Devices towards the TeraHertz Limit

E. Piccinini[1], F. Buscemi[2], M. Rudan[1], R. Brunetti[2], C. Jacoboni[2]

[1]DEI Department, University of Bologna, Viale Risorgimento 2, I-40136, Bologna, Italy
[2]FIM Department, University of Modena and Reggio Emilia, Via Campi 213/A, I-41125 Modena, Italy

E-mail: rossella.brunetti@unimore.it

Abstract. The time-dependent response of Ovonic devices to an electric potential ramp signal is analysed by means of an enhanced version of a previously published time-dependent charge-transport model proposed by the authors. Depending on the inevitable parasitics of the system, either stable or oscillating solutions are found according to the position of the load line. The model also allows for speculations on the potential of Ovonic materials in the design of high-frequency oscillating circuits close to the terahertz range.

1. Introduction

The topic of electrical and thermal transport in amorphous chalcogenides has been addressed several times in the last 40 years. A large community of scientists agrees in interpreting the steady-state, reversible switching behaviour of Ovonic materials as connected to hot-carrier phenomena [1, 2]. In particular, for given voltage biases, these semiconductors show the existence of two stable states featuring, on the microscopic scale, different carrier temperatures and, on the macroscopic scale, different resistivities, leading to the typical S-shaped current-voltage characteristic [2, 3, 4]. Most of the analyses published in the literature refer to steady-state conditions. Only recently some researchers pointed out that the investigation of the transient behaviour introduces new issues related to the switching time and to how the bias is applied [5]; others focused on the recovery time after the bias is changed [6].

The present work elaborates on the model by Buscemi *et al.* [7]. Thanks to the simplicity of the physical model, transport equations can be coupled to the circuit equation and used to describe transient situations with a limited computational load.

2. The model

According to a common framework for Ovonic materials, let us consider a homogeneous material, whose electron-state structure is extremely simplified and reduced to two distinct energy levels E_T and E_B, where $E_B = E_T + \Delta E_0$. The former level stands for the energy level of trapped carriers and the latter for that of mobile, or band, carriers. Since the mobility of trapped carriers is negligible, the current density reads $J = q\mu_B n_B F$, where n_B and μ_B are the concentration and the mobility of band carriers and F is the electric field.

The total concentration n of the carriers is fixed, but carriers can be differently distributed between the two levels depending on the transport conditions and on the applied electric field.

In particular, according to a Poole or Poole-Frenkel mechanism, the height of the energy barrier confining carriers in the traps depends on the electric field as $\Delta E_0 = \gamma |F|$, with γ a constant, so that the higher the applied field, the higher the probability of trapped carriers to transfer to band states. Given a field F, we assume that the steady-state band concentration $\tilde{n}_B$ can be expressed by the function [8]:

$$\tilde{n}_B = \frac{n}{1 + l \exp\left(\frac{\Delta E_0 - \gamma |F|}{kT_e}\right)}, \tag{1}$$

l being the ratio of the density of trap over band states, and T_e the electron temperature.
Under time-dependent conditions, the time evolution of the band population is assumed to vary as:

$$\frac{dn_B}{dt} = -\frac{n_B - \tilde{n}_B}{\tau_N}, \tag{2}$$

where τ_N is a relaxation time constant. This assumption makes n_B one of the unknowns of the problem and improves the model in [7], where n_B is instead instantaneously updated to $\tilde{n}_B$, which is a function of T_e.

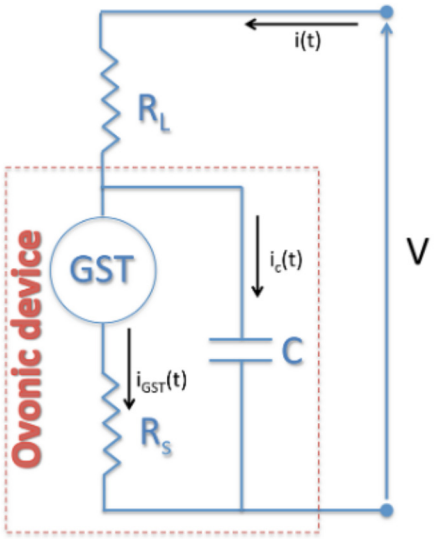

Figure 1. Schematics of the analyzed circuit. The boxed area represents an Ovonic device including the active layer and the parasitics. The capacitor C takes into account all capacitive parasitic effects, independently of their origin.

The time-dependent balance equation for the total energy density ε^{TOT} is written as:

$$\frac{d\varepsilon^{TOT}}{dt} = JF - \left.\frac{d\varepsilon^{TOT}}{dt}\right|_{lattice}, \tag{3}$$

where $\varepsilon^{TOT} = n_T E_T + n_B E_B = n_T E_T + n_B(E_T + \Delta E_0) = nE_T + n_B \Delta E_0$.

Coherently with the simplified model for the electron states, we assume for the energy relaxation due to the lattice [8]:

$$\left.\frac{d\varepsilon^{TOT}}{dt}\right|_{lattice} = n\frac{kT_e - kT_0}{\tau_T}. \tag{4}$$

with τ_T a relaxation time constant for T_e.

In order to exploit the above equations to study a device, we must consider a layer of Ovonic material between electrodes, giving rise to a parasitic capacitance C_S and a contact resistance R_S. Next, a series load resistance R_L and a parallel capacitance C_C due to the circuit are also considered. A schematic diagram of the circuit is sketched in Fig. 1 where the two capacitances have been replaced by the single capacitance $C = C_C + C_S$. The field F is not known *a-priori*, as it is a function of the circuit itself: $F = (V - R_L i)/(\ell + q\mu_B n_B A R_S)$, V being the external potential, ℓ and A being the device length and cross section, respectively.

The circuit theory leads to the following differential equation for the total current i:

$$\frac{di}{dt} = \frac{1}{CR_S R_L}\left[V - F\ell + CR_S\frac{dV}{dt} - i(R_S + R_L)\right], \tag{5}$$

which is coupled to (2) and (3) and solved numerically to find the triplet $\{n_B(t), i(t), T_e(t)\}$, given the external potential $V(t)$.

3. Results and discussion

Usual contact resistances and parasitic capacitances for Ovonic devices are hardly less than 1 kΩ and 1 pF, respectively [5, 6]. Following the literature, in the first part of our analysis we set $R_S = 1$ kΩ and $C = 1$ pF, and consider a large load resistance $R_L > 100$ kΩ, this rendering a current-driven circuit. When a simple bias, like a ramp signal to a voltage plateau V_{max}, is applied, three conditions are possibile, according to where the load line intersects the steady-state $I(V)$ characteristic (Figs. 2 and 3).

If the operating point lies in the lower branch of the $I(V)$ characteristic, a stable electric response is always reached, and the time needed to attain the steady-state condition depends both on the magnitude of the parasitic capacitance and, to a smaller extent, on the ramp slope. Similarly, a stable response is attained also when the load line crosses the upper branch of the $I(V)$ characteristic. In the latter case, a switching phenomenon takes place, and a current overshoot is present before the steady-state condition is reached (see Fig. 2).

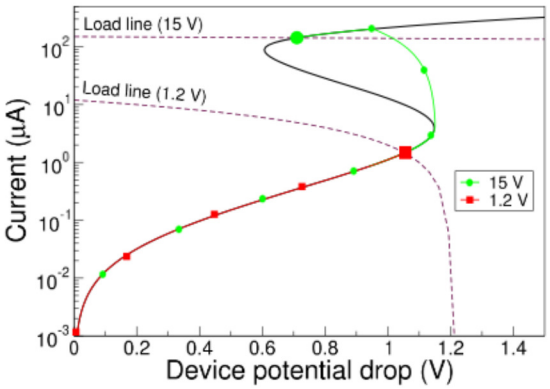

Figure 2. When the load lines intersects the steady-state $I(V)$ characteristic in the upper or lower branch, a stable state is found. The cases $V_{max} = 15$ V and $V_{max} = 1.2$ V, $R_L = 100$ kΩ are shown.

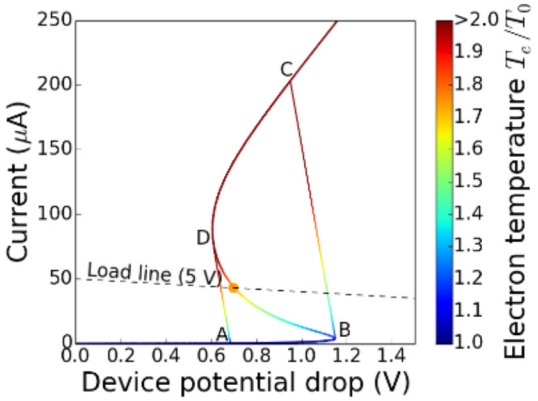

Figure 3. When the load line intersects the steady-state $I(V)$ characteristic in the NDR region ($V_{max} = 5$ V, $R_L = 100$ kΩ), the cycle $ABCD$ is found. Colors denote the electron temperature ratio T_e/T_0.

On the contrary, when the load line and the $I(V)$ characteristic intersect in the negative differential resistance region (NDR), the circuit becomes unstable and oscillations take place. In this case, the analyses of the time evolution of T_e helps in understanding how the cycle sets in. After the switching point is reached, T_e rapidly increases to values much higher than that of the operating point. Consequently, the current quickly jumps to high values. Due to (3), the contribution of energy relaxation is quite large, and eventually T_e jumps back to near-equilibrium values below the operating-point value. Then, the cycle starts again and continues to chase indefinitely the steady-state condition. The oscillating frequency found for these conditions is about 35 MHz. This value is similar to the one found in the literature [9], where the lower-to-upper branch transitions and v.v. are almost instantaneous.

The instability connected to the NDR branch of the $I(V)$ characteristic is a direct consequence of the presence of the parasitic capacitance C. In fact when C □ 0 it is found that the system reaches a stable condition in any case. Apart from any considerations on the parasitics due to probing and connections, we point out that a device with zero intrinsic capacitance cannot exist because of the two contacts necessary to generate the field inside the device.

One should also notice that, during the switching to the upper branch of the characteristic, T_e is always larger than the value it would have on the steady-state curve at the same current, and the opposite condition holds true while the system switches back to the lower branch (Fig.

3). Since such a behaviour is the result of the interplay between the parasitic capacitance and the two relaxation times τ_N and τ_T (here $\tau_N = 0.1$ ps and $\tau_T = 0.28$ ps), we can speculate on the oscillating frequency of the circuit, supposing that we are able to minimise the parasitic capacitance towards its theoretical limit. The smallest capacitance of a 1000 nm^2□40 nm capacitor with an Ovonic material as dielectric can be estimated in the order of $10^{\sqcup 3}$ fF.

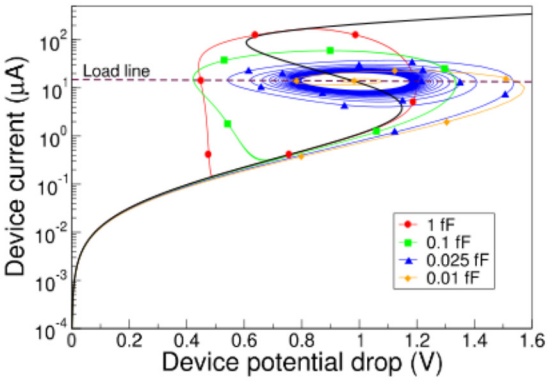

Figure 4. Simulations of the oscillating behaviour when the parasitic capacitance decreases from 1 fF down to $10^{\sqcup 2}$ fF. A plateau voltage $V_{max} = 15$ V and a load resistance $R_L = 1$ MΩ have been applied to set the working point in the NDR region.

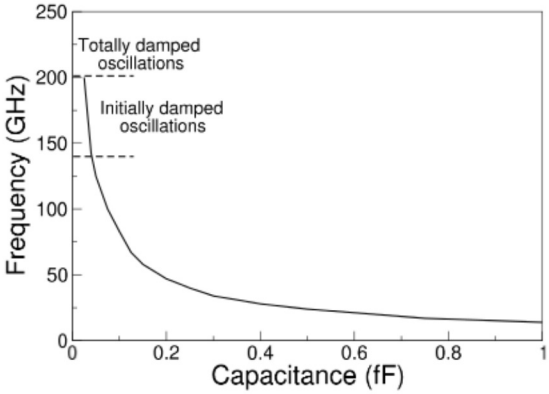

Figure 5. Oscillation frequencies for parasitic capacitances near the theoretical limit. Initially damped oscillations are reported for $0.025 < C < 0.04$ fF, while a totally damped behaviour is found below that limit.

In Fig. 4 we have simulated the circuit responses to a given bias for reduced parasitic capacitances, ranging from 1 fF down to $10^{\sqcup 2}$ fF, for an operating point lying in the NDR region. For the "largest" considered capacitances, the usual oscillations between the upper and the lower branches of the characteristic are found. Their frequencies are inversely proportional to C. However, as C decreases, the gap between the actual value of I_e and its "target" value at the same current reduces because the device approaches faster the steady-state conditions. In turn, changes on I_e imply changes of n_B, thus of i_{GST} and F. As a consequence, it may happen that progressively, high-frequency damped oscillations set in. Eventually, for further reductions of C, damping is so effective that the system converges to the operating point.

Performing a Fourier-transform of the voltage drop along the Ovonic device reveals that the maximum frequency that could be achieved is close to the terahertz domain (Fig. 5). This analysis suggests that Ovonic materials could be employed for high-frequency applications in the terahertz range, provided that technological advances do reduce circuit parasitics in such a way as to not overcome the intrinsic capacitance of the device as it happens today.

References

[1] Ielmini D 2008 **Phys. Rev. B 78** 035308
[2] Piccinini E, Cappelli A, Buscemi F, Brunetti R, Ielmini D, Rudan M, and Jacoboni C 2012 **J. Appl. Phys. 112** 083722
[3] Jacoboni C, Piccinini E, Buscemi F, and Cappelli A 2013 **Solid-State Electron. 84** 90
[4] Rudan M, Giovanardi F, Piccinini E, Buscemi F, Brunetti R, Cappelli A, Marcolini G, and Jacoboni C 2013 **J. Comput. Electron. 12** 666
[5] Wimmer M and Salinga M 2014 **New J. Phys. 16** 113044
[6] Lavizzari S, Ielmini D, and Lacaita A L 2010 **IEEE Trans. Electron. Dev. 57** 1838
[7] Buscemi F, Piccinini E, Brunetti R, Rudan M, and Jacoboni C 2014 **Appl. Phys. Lett. 104** 262106
[8] Buscemi F, Piccinini E, Cappelli A, Brunetti R, Rudan M, and Jacoboni C 2014 **Appl. Phys. Lett. 104** 022101
[9] Schmidt P E and Callarotti R C 1984 **J. Appl. Phys. 55** 3144